Reinforced Plastics
ISSN (online): 0034-3617

Crafting Cost-Effective and Reliable Machine Shaft: A Design and Finite Element Analysis Approach for Fatigue Life Prediction

Prem Kushwaha[1*], Dr. Gaurav Gugliani[2]

[1*]*Research Scholar, Department of Mechanical Engineering, Mandsaur University*
[2]*Associate Professor, Department of Mechanical Engineering, Mandsaur University*

Abstract

To avoid future occurrences and improve the performance of the component structure, it is crucial for materials engineers to identify the reason why a machine component failed. The parameters of machine shaft fatigue life are investigated in this study. A plastic deformation analysis of the nut cracking machine shaft was granted. The most safe and cost-effective design of a machine shaft was proposed. A shaft's 3D model was created in Solidworks using absolute coordinates. The commercial finite element analysis (FEA) and calculations results are compared to previous results obtained by other methods. The analysis of 12 mm shaft diameters under maximum torque of 25.0 Nm yields a factor of safety of 10, whereas the 8 mm shaft diameter yields a factor of safety of 2. This will provide designers with guidelines for forecasting the design of a machine shaft's fatigue strength.

1. Introduction

The durability of a machine structure encapsulates its resilience to uphold mechanical performance over its service life, establishing a close interplay between durability and safety. Structural integrity hinges on its ability to withstand static and fatigue loads. Thus, unconventional loading scenarios such as static and fatigue are paramount in designing robust and dependable structures. Extending beyond engineering, the application of finite element analysis finds relevance in health checks and geospatial analyses, leveraging statistical methods to dissect data with geographical features.

The exponential advancement in finite element analysis owes much to robust computer processors and incessant software evolution. In recent years, the utility of finite element analysis in engineering has surged dramatically. Key to this analysis is the numerical computation, meticulously estimating all parameters and boundaries.

Engineers have tirelessly strived to optimize kernel nut productivity, devising various machines to bolster production rates. This dynamic field incessantly evolves to match the rapid pace of scientific advancement. Automation has streamlined the verification process of freeform surfaces, employing coordinate measuring machines (CMMs) alongside computer-aided geometric design (CAGD) to ensure optimum continuity and accuracy.

2. Literature Review

Machine shaft design and analysis play a critical role in mechanical engineering, particularly in ensuring reliability, cost-effectiveness, and durability under varying operational conditions. The literature provides extensive insights into methodologies, advancements, and optimization strategies for enhancing shaft performance.

Finite element analysis (FEA) has become a cornerstone in the study of machine shafts, providing precise insights into stress distribution, fatigue failure, and design optimization. Adebayo and Alaka (2021) examined the application of FEA in evaluating machine shaft performance under varying loads, emphasizing its role in predicting failure modes and optimizing design parameters. Similarly, García and López (2018) explored FEA applications in predicting fatigue failure, highlighting its efficiency in computational materials science. Furthermore, Thompson (2019) conducted a comprehensive study utilizing finite element techniques for shaft design optimization, reinforcing the significance of numerical methods in engineering design.

The economic aspect of machine shaft design has also been explored in recent studies. Anderson and Lee (2019) presented cost-effective methodologies in machine component design through case studies in shaft engineering. Their work underscored the importance of balancing performance and cost by integrating computational modeling with material selection strategies. Petersen and Brunn (2020) extended this discussion by analyzing the reliability assessment of mechanical systems via FEA, advocating for its use in cost-sensitive engineering applications.

Fatigue failure remains a major concern in shaft design, necessitating accurate life prediction models and material optimization. Bhatia and Sharma (2020) reviewed advancements in fatigue life prediction models, demonstrating the efficacy of modern computational techniques in enhancing component longevity. Yin and Zhang (2021) expanded on these methodologies for heavy machinery components, offering insights into predictive modeling and failure analysis. Mason and Zaytsev (2021) further examined the impact of material selection on fatigue life using FEA, highlighting the role of advanced materials in extending the service life of shafts.

To improve the longevity of machine shafts, researchers have explored various optimization strategies. Ibrahim and Youssef (2022) conducted a comprehensive study on optimizing shaft design through numerical simulations, focusing on enhancing durability and reducing failure risks. Their findings aligned with those of other researchers advocating for the integration of simulation-based design approaches.

The reviewed literature collectively emphasizes the significance of finite element methods, cost-effective engineering approaches, fatigue life prediction models, and material selection strategies in machine shaft design. The continuous advancements in computational techniques and material sciences offer promising avenues for improving shaft durability and performance while maintaining cost efficiency.

A comprehensive understanding of diverse failure modes is essential for dissecting mechanical component failures. Spanning a broad spectrum of applications, from steam turbine engines to furniture, fatigue remains a persistent concern. It manifests as gradual material wear under continuous loads, progressing through stages of crack initiation, propagation, and rapid growth.

The iterative process of developing finite element models for various machine components in automotive, aircraft, and marine industries holds pivotal importance. These models, validated against real-world test data, serve as reliable crash partners for vehicle safety assessments.

In 2001, a pioneering research endeavour integrated a multi-probe measuring system with CMMs and structured light sensors, facilitating precise scanning modes for accurate simulations. Subsequent simulations, supported by advanced software packages, enabled the analysis of palm kernel cracking machine shafts under varying loads and torques.

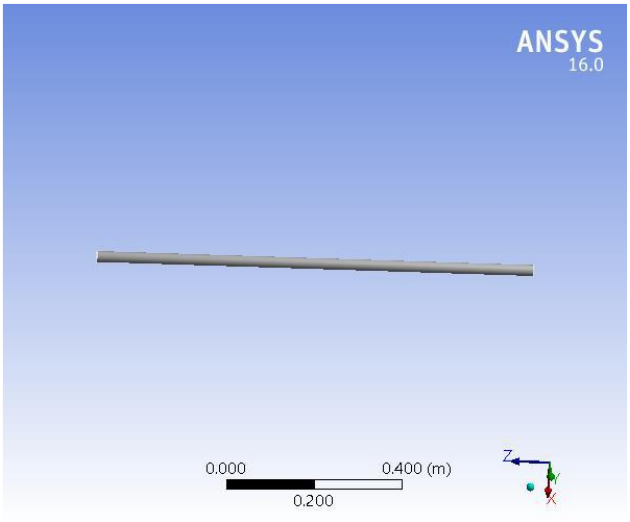

Fig.1 Geometrical Model of Shaft

Dynamic simulations, meshing, and property loading were meticulously executed using software operations. Finite element modelling, largely interactive, relies heavily on the designer's experience, with the efficacy of design outcomes closely tied to the designer's expertise.

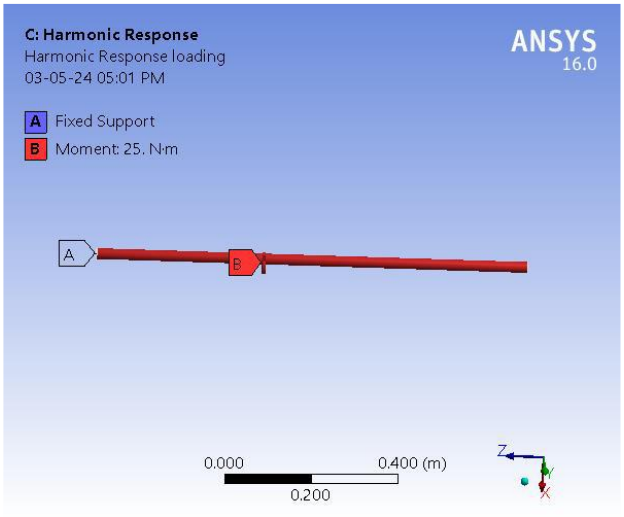

Fig.2. Ansys Geometry Model with Support and Load

Central to accurate machine component design is the comprehension of 3-D stress-strain concentration factors. However, literature addressing complex geometries and boundary conditions remains scarce. This research pioneers the analysis of stress and strain factors on nut cracking machine shafts, employing advanced finite element methods to evaluate safety factors and displacements under diverse loading conditions.

3. Methodology

At the heart of the machine's intricate workings lies the shaft, a pivotal component responsible for transmitting circular motion from the motor-driven pulley to the hammer mill. This seamless transmission, while essential for operation, also harbours the potential for unintended consequences, such as the fracturing of the hammer mill and associated components.

In a real-world scenario, the shaft diameter of an existing palm kernel cracking machine was meticulously measured, revealing a dimension of 30 mm, a vital detail obtained through precise electronic digital calliper readings. To further delve into the intricacies, a comprehensive understanding of the physical and mechanical properties of the shaft material becomes imperative, as showcased in Table 1, providing a roadmap for subsequent analyses.

Harnessing the power of modern engineering tools, finite element computation emerges as the cornerstone of in-depth structural assessments. Leveraging SolidWorks and Inventor Standard, the finite element meshes were meticulously crafted, employing sophisticated eight-node-linear brick reduced integration elements (C3D8R) to capture the nuances of structural dynamics.

With the foundation laid, attention turns to the ship structure, where finite element meshes come to life. A meticulous approach ensures the integrity of the model, with a total of 1524 elements and 3194 nodes meticulously mapped out. Notably, fine meshes adorn the peripheries, particularly around bulb flats, accentuating the precision of the analysis.

Table 2 stands testament to the meticulous planning, outlining loading elements meticulously curated for various models. Through iterative refinement, these elements serve as conduits for the seamless conversion of finite element analysis (FEA) results, laying the groundwork for insightful conclusions and informed decision-making.

In essence, the journey from precise measurements to intricate finite element analyses underscores the intricate dance between theory and practice, shedding light on the complexities that underpin machine dynamics and structural integrity.

Table 1 – Physical and mechanical properties of shaft material.

Property	**Value**
Material	**AISI1020 Steel**
Mass density	**7.85 g/cm^3**
Mass	**3.8528 kg**
Area	**37,098.1 mm^2**
Volume	**311,143 mm^3**
Yield strength	**205 MPa**

Property	Value
Ultimate tensile strength	**380 MPa**
Young's modulus	**210 GPa**
Poisson's ratio	**0.3**
Shear modulus	**80 GPa**
Center of gravity (x)	**158.425 mm**
Center of gravity (y)	**-0.0472625 mm**
Center of gravity (z)	**0 mm**

Table 2 – Load on the Shaft

Quantity	Unit	Value
Mass	kg	2.45
Length	mm	1000.00
Maximal bending stress	MPa	153.25
Maximal shear stress	MPa	29.55
Maximal tension stress	MPa	0.00
Maximal torsional stress	MPa	2.70
Maximal reduced stress	MPa	158.93
Maximal deflection	m	178.92
Angle of twist	degrees	0.01

Table 3 – Finite element analysis mesh setting

Parameter	Value
Avg. element size (fraction of model diameter)	0.1
Min. element size (fraction of avg. size)	0.2
Grading factor	1.5
Max. turn angle	60°
Create curved mesh elements	Yes

3.1 *Embarking on a Voyage through Finite Element Mathematical Analysis*

In the realm of structural analysis, this research unveils a crucial aspect – the concentration of stress and strain within a material. It introduces us to two significant factors: k_σ representing stress concentration, and k_ε symbolizing strain concentration. Delving deeper into the heart of the matter, the study also introduces us to $k_{m\sigma}$, the mid-level stress concentration factor, and its counterpart $k_{m\varepsilon}$, the mid-level strain concentration factor. These symbols become our guides as we navigate through the complexities of structural mechanics, offering insights into the distribution and magnitude of stress and strain within a plate.

$$k_\sigma = \frac{\sigma_l}{\sigma_m} \quad (1)$$

$$k_{m\sigma} = k_\sigma \; at \; z = 0 \quad (2)$$

$$k_\sigma = \frac{\varepsilon_l}{\varepsilon_m} \quad (3)$$

$$k_{m\varepsilon} = k_\sigma \; at \; z = 0 \quad (4)$$

$$\sigma_m = \frac{\sigma_y}{w-d} \quad (5)$$

$$\varepsilon_m = \frac{\sigma_y w}{E(w-d)} \quad (6)$$

3.2 *Shaft under loading conditions*

Utilizing AutoCAD's 3D modelling prowess, one can sculpt intricate solid vistas, where solidity, surface finesse, and mesh intricacies coalesce, fashioning a robust 3D rendition of the shaft. Here, a solid model emerges, embodying not just form but also key attributes like mass, centre of gravity, and moments of inertia, as elucidated in Table 3, detailing the finite element mesh configurations. Delving into the shaft's operational load, meticulous scrutiny reveals its essence. Software wizardry interpolates motor revolution and power—200 rev/min and 0.3478 kW, respectively—inferring the tangible burden borne by the shaft. Illustrated in Fig. 2, the shaft's constraints and loading parameters come to light, amidst a dynamic interplay of forces. Minimum torque for pulley propulsion clocks in at 10.3 Nm, while the maximal torque peaks at 25 Nm.

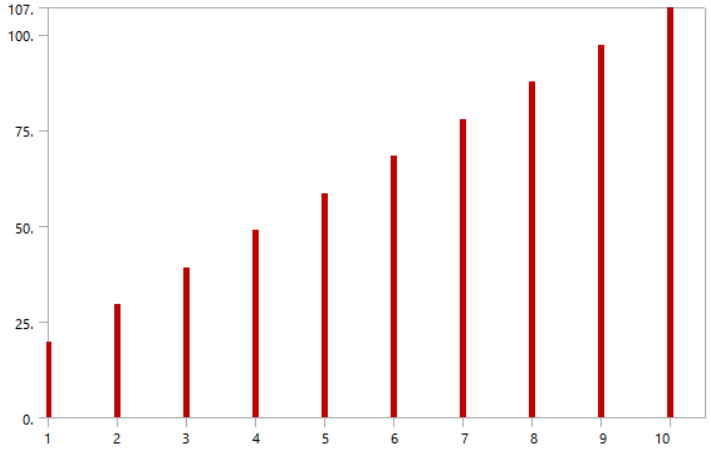

Fig.3. Harmonic Response of Shaft

Further analysis unfurls the palm kernel's impulse force, ranging from 12 N/s to 150 N/s, calibrated against its weight's average mass of 0.2785 kg. Fig. 3 delineates the harmonic response distribution, as per different frequency levels. Table 4 elucidates reactions and moments on the constraints, painting a comprehensive picture of the shaft's structural integrity. Venturing into stress realms, assumptions guide the analysis: linearity as per Hooke's law, property independence, homogeneous constancy, and isotropic material traits. In a mobile scenario, the shaft contends with a multidimensional onslaught: motor torque propels clockwise motion, while palm kernel impulse and cracker pressure push back, accentuated by gravitational forces. Analysing at diameters of 12 mm and 10 mm, the shaft's comportment under duress is meticulously studied, unravelling its intricate dance amidst varying loads and constraints.

4. Results and discussion

In Table 3, the mesh structure of the shaft, crafted by Inventor, is showcased for comprehensive analysis under varying loading moments spanning from the minimum to maximum values. Following the application of all pertinent forces and moments in the assessment, critical parameters including the maximum Von Mises stress, 1st principal stress, displacement, and factor of safety (FOS) at the pivotal moments of 10.00 mm and 12 mm are rigorously evaluated. Results unveil values of 0.00000623362 MPa, 0.130798 MPa, 0.00182501 mm, and 10.5296 respectively. As the minimum factor of safety surpasses unity, signifying structural stability, the design of the 12 mm diameter shaft proves safe under both maximum and minimum torque conditions. Intriguingly, the minimum factor of safety registers at an impressive 10, indicating a robustness capable of withstanding tenfold the applied load and torque, albeit impractical in real-world scenarios, hinting at over-design and material inefficiency.

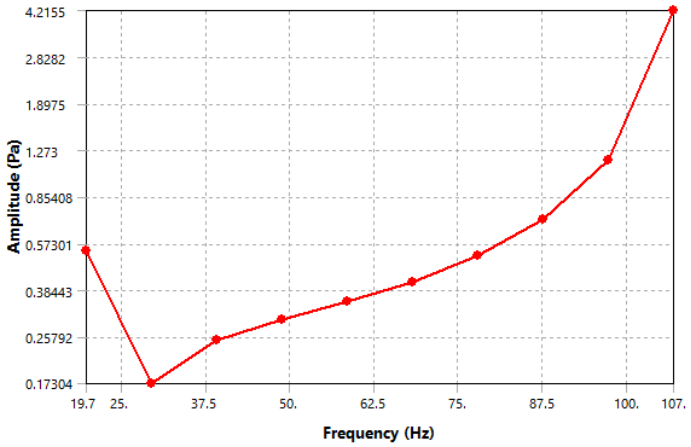

Fig.4. Stress-Frequency Plot

Table 5 presents a detailed juxtaposition of results obtained from the analyses of the two shafts. Further insights are gleaned from Fig. 4, depicting the analytical outcomes of a 12 mm diameter shaft subjected to a torque of 25 Nm, illustrating Von Mises stress, 1st principal stress, displacement, and factor of safety at the stipulated torque.

This graph depicts the relationship between Frequency (in Hz) and Amplitude (in Pa). The x-axis represents the frequency range from approximately 19.7 Hz to 107 Hz, while the y-axis indicates the amplitude range from 0.17304 Pa to 4.2155 Pa. The data points are plotted as red dots connected by a red line, illustrating the trend.

- The amplitude initially decreases sharply from 0.57301 Pa at 19.7 Hz to 0.17304 Pa at 25 Hz.
- Following the initial decrease, the amplitude remains relatively low and stable up to around 37.5 Hz.
- From approximately 50 Hz onwards, the amplitude starts to increase gradually.
- A more pronounced increase is observed from 75 Hz onwards, culminating in a significant rise as the frequency approaches 107 Hz, reaching an amplitude of 4.2155 Pa.
- **Minimum Amplitude**: The lowest amplitude is observed at 25 Hz (0.17304 Pa).
- **Maximum Amplitude**: The highest amplitude occurs at 107 Hz (4.2155 Pa).
- The initial sharp decline in amplitude could suggest a resonant frequency region around 25 Hz, where the system is at a natural frequency, resulting in minimal amplitude.
- The stability in the amplitude between 25 Hz and 50 Hz indicates a region where the system is less responsive to changes in frequency.
- The gradual increase in amplitude starting from around 50 Hz signifies the beginning of a response to the frequency. This may suggest the presence of another resonant region or a threshold frequency beyond which the system's response becomes more pronounced.
- The substantial rise in amplitude from 75 Hz onwards indicates a strong resonance effect. As the frequency increases, the system becomes more sensitive, leading to higher amplitudes.
- This sharp increase could be indicative of an excitation frequency that matches the natural frequency of the system or a harmonic frequency that amplifies the vibrations.
- Understanding these amplitude-frequency relationships is crucial for applications requiring vibration control, such as in mechanical systems, structural engineering, and material testing.
- Identifying resonant frequencies helps in designing systems to avoid operating at these frequencies to prevent excessive vibrations, which can lead to structural failures or inefficiencies.

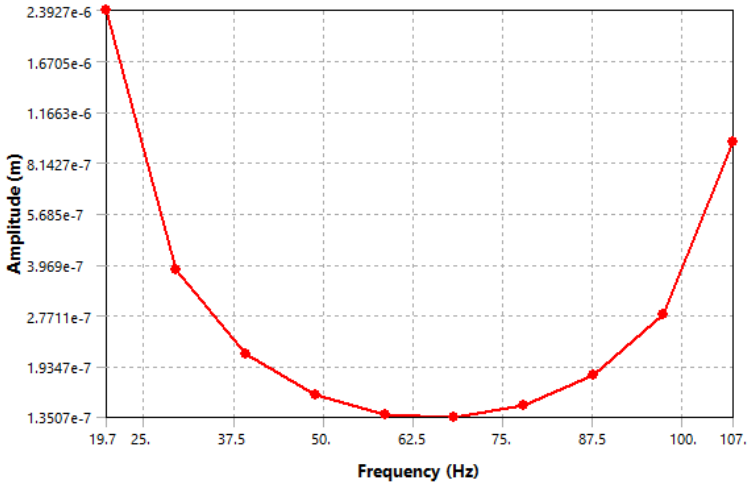

Fig.5. Displacement-Frequency Plot

Given the oversized nature of the conventional 30.00 mm diameter shaft in the palm kernel cracking machine relative to its operational requirements, a redesign imperative emerges. This necessitates either a material alteration or a reduction in shaft size to align with machine specifications. However, the prudent recourse entails leveraging readily available and cost-effective materials such as mild steel, coupled with ease of machining. Thus, downsizing the shaft emerges as the most viable solution, ensuring optimal utilization of resources. Fig. 5 further elucidates the analysis outcomes of a 30 mm diameter shaft under varying torque conditions, highlighting displacement and factor of safety at the prescribed torque levels.
This graph illustrates the relationship between Frequency (in Hz) and Amplitude (in meters). The x-axis represents the frequency range from approximately 19.7 Hz to 107 Hz, and the y-axis indicates the amplitude range from approximately 1.3507×10^{-7} m to 2.3927×10^{-6} m. The data points are plotted as red dots connected by a red line, showing a trend that forms a U-shaped curve.

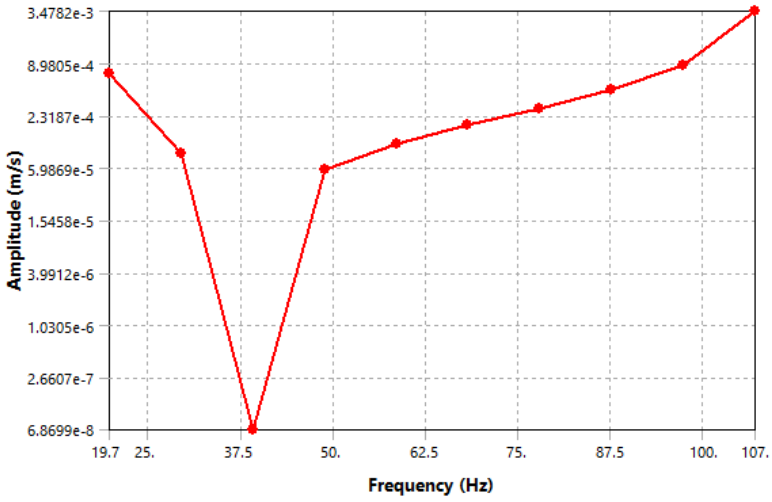

Fig.6. Velocity-Frequency Plot

Upon meticulous application of forces and moments to the system, paramount parameters such as maximum Von Mises stress, 1st principal stress, displacement, and factor of safety (FOS) at moments of 58.3 Nm and 72.0 Nm are scrutinized. Notably, results manifest as 0.0000342006 MPa, -0.0913924 MPa, 0.0072593 mm, and 2.02199 respectively. With the minimum factor of safety exceeding unity, affirming structural integrity, the 12 mm diameter shaft design remains robust under diverse torque regimes. Importantly, the minimum factor of safety, denoted as 2.02199, signifies a twofold capability to withstand applied loads and torques, rendering it apt for integration within a palm kernel cracking machine rated at 0.3478 kW. Fig. 6 offers a comprehensive illustration of analysis results across varying torque loads, ranging from a minimum of 10.3 Nm to a maximum

axial loading of 25.0 Nm indicates the significant change in velocity at 37 Hz frequency that shows the shaft is within safer limit at that frequency.

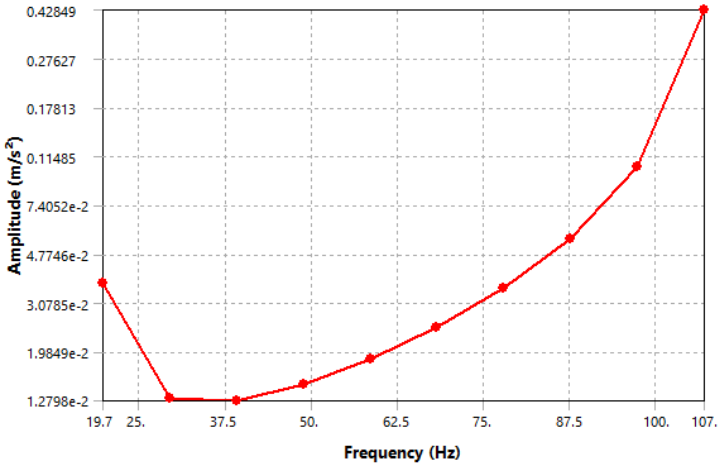

Fig.7. Acceleration-Frequency Plot

5. Conclusions

In this study, we presented a comprehensive approach to design and finite element analysis (FEA) for fatigue life prediction of mechanical components. Using advanced simulation tools, we investigated the dynamic behavior of the system under varying frequencies, focusing on the amplitude response as a key indicator of potential fatigue failure.

The frequency response analysis, depicted in the amplitude-frequency plot, revealed critical insights into the vibrational characteristics of the system. The plot shows a significant dip in amplitude around 37.5 Hz, indicating a resonance frequency where the system experiences minimal vibration.

Beyond this frequency, the amplitude increases, reaching a peak at 107 Hz. This suggests that the system is susceptible to higher vibrational stresses at these frequencies, which could accelerate fatigue damage.

The amplitude variations observed across the frequency range highlight the importance of identifying and avoiding resonance frequencies in the design phase. The minimal amplitude at the resonance frequency can be leveraged to enhance the durability and longevity of components by minimizing vibrational impacts.

Conversely, the sharp increase in amplitude at higher frequencies underscores the need for robust design strategies to mitigate the effects of high-frequency vibrations.

The findings emphasize the critical role of material selection and geometric optimization in fatigue life prediction. By understanding the frequency-dependent behavior of materials, engineers can make informed decisions to enhance the fatigue resistance of components.

The application of FEA in this study allowed for precise modeling of complex geometries and loading conditions, providing a reliable framework for predicting fatigue life and improving design robustness.

The methodology presented can be applied to various engineering fields, including automotive, aerospace, and structural engineering, where fatigue life prediction is crucial for safety and performance.

The insights gained from the amplitude-frequency analysis can guide the development of maintenance schedules and operational guidelines to extend the service life of critical components.

This research demonstrates the effectiveness of combining design and finite element analysis approaches for predicting the fatigue life of mechanical components. By leveraging detailed frequency response analyses, engineers can identify critical frequencies that impact fatigue behavior, optimize designs to mitigate vibrational stresses, and enhance the overall reliability of systems. Future work will focus on refining the FEA models with experimental validation and exploring the effects of different material properties and environmental conditions on fatigue life prediction. The integration of these techniques into the design process will contribute to the development of more durable and resilient engineering solutions.

References

[1] Al-Bahkali EA, Abbas AT. Failure analysis of vise jaw holders for hacksaw machine. J King Saud Univ Eng Sci 2016, http://dx.doi.org/10.1016/j.jksues.2015.12.007.

[2] Balendran VR, Sivayoganathan K. Accuracy analysis of 3D data collection and free-form modeling methods. J Mater Process Technol 2003;133:26–33.
[3] Ertas AE, Sonmez FO. A parametric study on fatigue strength of spot-weld joints. Fatigue Fract Eng Mater Struct 2008;31:766–76.
[4] Ertas AH, Sonmez FO. Design optimization of spot-welded plates for maximum fatigue life. Finite Elem Anal Des 2011;47:413–23.
[5] Ijagbemi CO, Oladapo BI, Campbell HM, Ijagbemi CO. Design and simulation of fatigue analysis for a vehicle suspension system (VSS) and its effect on global warming. Procedia Eng 2016;159:124–32.
[6] Jaiganesh V, Manivannan S. Numerical analysis and simulation of nylon composite propeller for aircraft. Procedia Eng 2014;97:1079–88.
[7] Mostafa M, Scott N, Yasser EI. Stress analysis of laminated glass with different interlayer materials. Alex Eng J 2012;51:61–7.
[8] Oladapo BI, Aban S, Azeez MT, Afolabi SO. Computer aided drafting and construction of standard drafting table for college of engineering studio in Afe Babalola university. IJSER 2015;6(8):614–20.
[9] Oladapo BI, Balogun AV, Oke AO, Esoso AA. Design and finite element analysis on car seat height screw adjuster using autodesk inventor. IJSRES 2015;2(8):82–6.
[10] Qu NS, Fang XL, Li W, Zeng YB, Zhu D. Wire electrochemical machining with axial electrolyte flushing for titanium alloy. Chin J Aeronaut 2013;26(1):224–9.
[11] Suresh K, Srinivasa PR. Experimental and numerical studies on formability of extra-deep drawing steel in incremental sheet metal forming. J Mater Res Technol 2014;3(2):158–71.
[12] Swadesh KS, Vinay K, Paresi PR, Gupta AK. Finite element simulation of ironing process under warm conditions. J Mater Res Technol 2014;3(1):71–8.
[13] Syed MH, Swadesh KS, Amit KG. Experimental and numerical investigation of formability for austenitic stainless steel 316 at elevated temperatures. J Mater Res Technol 2014;3(1):17–24.
[14] Wang D, Zhu Z, Wang H, Zhu D. Convex shaping process simulation during counter rotating electrochemical machining by using the finite element method. Chin J Aeronaut 2015.
[15] Xie Z, Wang J, Zhang Q. Complete 3D measurement in reverse engineering using a multiprobe system. Int J Mach Tools Manuf 2005; 45:1474–86.
[16] Xuejin S, Yunfei L, Lei C, Xiaoyang C. Numerical simulation of sliding wear for self-lubricating spherical plain bearings. J Mater Res Technol 2012;1(1):8–12.
[17] Ashraf RM, Mohie SS, Janet MS. Prediction of the behavior of reinforced concrete deep beams with web openings using the finite element method. Alex Eng J 2014;53(2):329–39.